Nonlinear excitations in the classical one-dimensional antiferromagnet

M. E. Gouvea and A. S. T. Pires
Departamento de Física, Universidade Federal de Minas Gerais, Belo Horizonte, MG, 30000, Brazil
(Received 21 May 1985)

In this paper we study nonlinear excitations in the classical one-dimensional antiferromagnet with two anisotropies and an external magnetic field with components parallel and perpendicular to the chain. We use the continuum approximation, at low temperatures, to obtain two coupled nonlinear equations in the variables θ and Φ, and then we discuss some limit solutions to these equations. We study the equivalence of this model, from the thermodynamical point of view, to an anisotropic ferromagnet whose statistical mechanics has been studied in the literature. We then use this equivalence to calculate the inverse correlation length, the neutron scattering intensity integrated over energy, the soliton density, and the soliton energy. Our theory is found to be in good agreement with experimental data for tetramethyl ammonium trichloride [TMMC,$(CD_3)_4NMnCl_3$].

I. INTRODUCTION

Recently there has been a great interest in the study of nonlinear solutions to the equations of motion associated with one-dimensional classical magnetic systems.[1] Although most of the work has been done for the sine-Gordon chain,[2] some authors have studied the full equation of motion for the magnetic chain. Sasaki,[3] Etrich and Mikeska,[4] and Fogedby *et al.*[5] have studied the statistical mechanics of a classical Heisenberg ferromagnet with two anisotropies. Other authors have considered the ferromagnet[6–11] and the antiferromagnet[12–14] with one anisotropy in an external magnetic field. In this paper we will present a theoretical investigation of nonlinear excitations in a classical one-dimensional anisotropic antiferromagnet in an external field. Leung *et al.*[15] have studied sine-Gordon solitons in this system and Mikeska[13,14] has considered the equations of motion for the full Hamiltonian in some particular cases.

As pointed out by Leung *et al.*[15] solitons in quasi-one-dimensional antiferromagnets are of interest for several reasons. First, in most one-dimensional magnetic salts, the exchange coupling is antiferromagnetic. Also, the solitons in the ferromagnet and the antiferromagnet have very different properties. For instance, much larger magnetic fields are required to drive the antiferromagnet into the regime where the soliton rest energy is large compared to k_BT and the solitons form a dilute gas of noninteracting elementary excitations.

In fact, we will be interested in the antiferromagnet tetramethyl ammonium trichloride (TMMC), which has an anisotropy of dipolar origin $\delta S_n^z S_{n+1}^z$ leading the system to a crossover to the XY model at low temperatures,[16] and a single-ion anisotropy in the easy plane.[17,18]

In Sec. II, we present the classical equations of motion for our general model and discuss some particular solutions. In Sec. III, we study the statistical mechanics of the system. Section IV is devoted to comparison between our theory and experimental data for TMMC.

II. EQUATIONS OF MOTION

Let us start with a general model described by the following Hamiltonian,

$$\mathscr{H}=2J\sum_n[\mathbf{S}_n\cdot\mathbf{S}_{n+1}-\delta S_n^zS_{n+1}^z+b_1(S_n^x)^2+b_2(S_n^y)^2]-\gamma H_x\sum_n S_n^x-\gamma H_z\sum_n S_n^z\ , \tag{2.1}$$

where $\gamma=g\mu_B$. At low temperature and for small anisotropies, $(S_n^\alpha)^2$ has the same effect as $-S_n^\alpha S_{n+1}^\alpha$, and our Hamiltonian (2.1) is completely general.

For small magnetic fields we expect that two neighboring spins are almost antiparallel to each other at low temperatures. Following Mikeska[13] and Harada *et al.*,[12] we introduce angle variables as

$$\mathbf{S}_n=(-1)^nS(\sin[\theta_n+(-1)^nv_n]\sin[\Phi_n+(-1)^n\phi_n]\ ,\cos[\theta_n+(-1)^nv_n],\sin[\theta_n+(-1)^nv_n]\cos[\Phi_n+(-1)^n\phi_n])\ , \tag{2.2}$$

and substitute them into (2.1). Since v and ϕ as well as the spatial variation of θ and Φ are expected to be small, we keep only the terms up to the second order of those small quantities. Using the continuum approximation, we obtain

$$\mathscr{H}=JS^2\int\frac{dz}{a}\left\{\left[\frac{\partial\theta}{\partial z}\right]^2+4v^2+\sin^2\theta\left[4\phi^2+\left[\frac{\partial\Phi}{\partial z}\right]^2\right]+2(\delta\cos^2\Phi+b_1\sin^2\Phi)\sin^2\theta\right.$$
$$\left.+2b_2\cos^2\theta-4\phi\sin\theta(h_x\cos\Phi-h_z\sin\Phi)-4v\cos\theta(h_x\sin\Phi+h_z\cos\Phi)\right\}\ , \tag{2.3}$$

where $h_\alpha=\gamma H_\alpha/4JS$, z is the coordinate along the chain, and a is the lattice constant.

The equations of motion can be obtained either directly, by applying the continuum approximation to the equation of motion on the discrete lattice, or from Hamiltonian (2.3). We obtain

$$\frac{1}{4JS}\frac{\partial\theta}{\partial t}=2\phi\sin\theta+(\delta+b_1)v\cos\theta\sin\Phi\cos\Phi-h_x\cos\Phi+h_z\sin\Phi\ , \tag{2.4}$$

$$\frac{1}{4JS}\frac{\partial\Phi}{\partial t}=-\frac{2v}{\sin\theta}+\delta v\cos^2\Phi\frac{1+\cos^2\theta}{\sin\theta}+h_x\cot g\theta\sin\Phi+h_z\cot g\theta\cos\Phi$$
$$-b_2v\sin\theta-b_1\phi\cos\theta\sin\Phi\cos\Phi+\frac{b_1v}{2}\sin\theta\sin^2\Phi\ , \tag{2.5}$$

$$\frac{1}{4JS}\frac{\partial v}{\partial t}=-2v\phi\cos\theta-\cos\theta\frac{\partial\theta}{\partial z}\frac{\partial\Phi}{\partial z}-\tfrac{1}{2}\sin\theta\frac{\partial^2\Phi}{\partial z^2}-(\delta-b_1)\sin\theta\sin\Phi\cos\Phi+h_x\phi\sin\Phi+h_z\phi\cos\Phi\ , \tag{2.6}$$

$$\frac{1}{4JS}\frac{\partial\phi}{\partial t}=\frac{2v^2\cos\theta}{\sin^2\theta}-2\phi^2\cos^2\theta-\tfrac{1}{2}\cos\theta\left[\frac{\partial\Phi}{\partial z}\right]^2+\frac{1}{2\sin\theta}\frac{\partial^2\theta}{\partial z^2}-\delta\cos\theta\cos^2\Phi-\frac{v}{\sin^2\theta}(h_x\sin\Phi+h_z\cos\Phi)$$
$$+\phi\frac{\cos\theta}{\sin\theta}(h_x\cos\Phi-h_z\sin\Phi)+b_2\cos\theta-b_1\cos\theta\sin^2\Phi\ . \tag{2.7}$$

After eliminating the small angles ϕ and v, we find

$$\frac{\partial^2\theta}{\partial z^2}-\frac{1}{c^2}\frac{\partial^2\theta}{\partial t^2}=\sin\theta\cos\theta\left[\left[\frac{\partial\Phi}{\partial z}\right]^2-\frac{1}{c^2}\left[\frac{\partial\Phi}{\partial t}\right]^2\right]-\frac{\sin^2\theta}{2JS}(h_x\sin\Phi+h_z\cos\Phi)\frac{\partial\Phi}{\partial t}$$
$$+\sin\theta\cos\theta[(h_x\sin\Phi+h_z\cos\Phi)^2+2b_1\sin^2\Phi+2\delta\cos^2\Phi-2b_2]\ , \tag{2.8}$$

$$\frac{\partial^2\Phi}{\partial z^2}-\frac{1}{c^2}\frac{\partial^2\Phi}{\partial t^2}=-2\cot g\theta\left[\frac{\partial\theta}{\partial z}\frac{\partial\Phi}{\partial z}-\frac{1}{c^2}\frac{\partial\theta}{\partial t}\frac{\partial\Phi}{\partial t}\right]+\frac{h_x\sin\Phi+h_z\cos\Phi}{2JS}\frac{\partial\theta}{\partial t}+\sin\Phi\cos\Phi(h_x^2-h_z^2+2b_1-2\delta)\ , \tag{2.9}$$

where $c=4JSa$. For $b_1=b_2=0$, $h_z=0$, Eqs. (2.8) and (2.9) are equivalent to the ones obtained by Flüggen and Mikeska,[14] noting that we have used a different coordinate system.

The general solutions of Eqs. (2.8) and (2.9) are very difficult to obtain. Thus we will only consider some special cases and soliton solutions. Let us first study the problem for a null external magnetic field. If $b_2<b_1$ and $b_2<\delta$, the ground state is along the y direction. Since for this case $\Phi=0$ and $\Phi=\pi/2$ satisfies the full Eqs. (2.8) and (2.9), complete dynamical solutions are obtained from

$$\Phi=0,\quad \frac{\partial^2\theta}{\partial z^2}-\frac{1}{c^2}\frac{\partial^2\theta}{\partial t^2}=2(\delta-b_2)\sin\theta\cos\theta\ , \tag{2.10}$$

$$\Phi=\frac{\pi}{2},\quad \frac{\partial^2\theta}{\partial z^2}-\frac{1}{c^2}\frac{\partial^2\theta}{\partial t^2}=2(b_1-b_2)\sin\theta\cos\theta\ . \tag{2.11}$$

These are sine-Gordon equations in the variable 2θ; the fully dynamical yz and yx solitons are therefore given by

$$\theta=\frac{\pi}{2}+2\arctan[\exp\sqrt{k}\,\gamma(z-ut)]\ , \tag{2.12}$$

with energy

$$E=4JS^2\sqrt{k}\,\gamma\ , \tag{2.13}$$

where $\gamma=(1-u^2/c^2)^{-1/2}$ and $k=2(\delta-b_2)$ for yz solitons, and $k=2(b_1-b_2)$ for yx solitons. Depending on the ratio $r=(\delta-b_2)/(b_1-b_2)$, the yz soliton ($r<1$, easy yz plane) or the yx soliton ($r>1$, easy yx plane) has lower energy. From a linear stability analysis, we obtain the result that the lower-energy soliton is stable with respect to small perturbations. For $r=1$ (i.e., $\delta=b_1$), there is rotational degeneracy. That is, we have a dynamic sine-Gordon soliton for any $\Phi=\Phi_0=$const. In this case, Hamiltonian (2.1) is equivalent to the Hamiltonian for an Ising-like antiferromagnetic chain. Thus the picture for the nonlinear dynamics for this case is the following: There are always two sine-Gordon branches. For $\delta=b_1$, these two modes become degenerate.

If $h=0$ but $b_1<b_2$, $b_1<\delta$, the ground state is now along the x direction. As we can see, $\Phi=\pi/2$, the xy soliton, is still a solution. The other solution is given by

$$\theta=\frac{\pi}{2},\quad \frac{\partial^2\Phi}{\partial z^2}-\frac{1}{c^2}\frac{\partial^2\Phi}{\partial t^2}=-2(\delta-b_1)\cos\Phi\sin\Phi\ . \tag{2.14}$$

The soliton solution of Eq. (2.14) is an xy sine-Gordon soliton in the variable 2Φ with energy $E=4JS^2\gamma(\delta-b_1)^{1/2}$. For $\delta=b_2$, there is rotational degeneracy for dynamical sine-Gordon solitons in any plane passing through the x axis. Similarly, we can study any other case, such as, for instance, $\delta<b_1\le b_2$.

Let us now consider the case where the magnetic field is perpendicular to the chain (i.e., the H_x component). As far as static properties are concerned, the effect of the magnetic field is to introduce an effective anisotropy given by $h_x^2/2$. However, from the dynamical point of view, a magnetic field is not equivalent to an anisotropic term. Let us start with the case $b_2<\delta$, $b_2<b_1+h_x^2/2$.

The ground state is along the y direction. As we can see, the dynamical yz soliton [$\Phi=0$, Eq. (2.10)] is still a solution. Then the magnetic field has no effect in this mode. We also find immediately that $\Phi=\pi/2$ is a static solution, the equation for θ being

$$\frac{\partial^2\theta}{\partial z^2}=2(h_x^2/2+b_1-b_2)\sin\theta\cos\theta \ . \tag{2.15}$$

Thus the static soliton solution is given by

$$\theta_0=2\arctan[\exp(h_x^2+2b_1-2b_2)^{1/2}z] \ , \tag{2.16}$$

with energy

$$E_{xy}^0=4JS^2(h^2+2b_1-2b_2)^{1/2} \ . \tag{2.17}$$

A complete time-dependent solution for the xy soliton cannot be obtained analytically. However, for small velocities, we can take, following Ref. 14,

$$\theta_{xy}(z,t)=\theta_0 \ , \tag{2.18a}$$

$$\Phi_{xy}(z,t)=\frac{\pi}{2}+u\phi_1(s) \ , \tag{2.18b}$$

where $s=z-ut$. Inserting Eqs. (2.18) into Eq. (2.9), we find the equation

$$\frac{1}{\tilde{h}^2}\frac{d^2\phi_1}{ds^2}+\left[1-\frac{2(\delta-b_2)+h_z^2}{\tilde{h}^2}\right]\phi_1+\frac{2}{\tilde{h}}\tanh(\tilde{h}s)\frac{d\phi_1}{ds}=-\frac{h_x}{\tilde{h}}\frac{1}{2JS}\mathrm{sech}(\tilde{h}s) \ , \tag{2.19}$$

where

$$\tilde{h}=[h_x^2+2(b_1-b_2)]^{1/2} \ .$$

Equation (2.19) has the solution

$$\phi_1(s)=(R/2JS)\mathrm{sech}(\tilde{h}s) \ , \tag{2.20}$$

where

$$R=\frac{\tilde{h}h_x}{2(\delta-b_2)+h_z^2} \ . \tag{2.21}$$

The u^2 correction to the energy can be calculated using Eq. (2.20). For small values of R we find

$$E_{xy}\simeq E_{xy}^0\left[1+\frac{u^2}{c^2}\left[\frac{1}{2}+\frac{4}{3\lambda}\right]\right] \ , \tag{2.22}$$

where

$$\lambda=R^{-1}-1 \ . \tag{2.23}$$

For $b_1=b_2=0$, $h_z=0$, Eq. (2.22) agrees with the result obtained in Ref. 14.

We could also study the case for large R, but we are interested here in corrections to the sine-Gordon model, and for large R, the system behaves like an Ising model. Summarizing, we see that for $u=0$, the soliton is in the xy plane. For a non-null velocity, the soliton moves out of this plane. If $R<1$, we have $E_{xy}^0<E_{yz}^0$. The energy E_{xy} increases with u, the soliton being stable against small perturbations.

If $h_x^2+2b_1=2\delta$, the yz soliton is the only dynamical soliton solution. The xy soliton is a degenerate static solution. That is, a static soliton in any plane $\Phi=$const is a degenerate solution with energy

$$E_0=E_{yz}^0=4JS^2[2(\delta-b_2)]^{1/2} \ . \tag{2.24}$$

The curvature of the xy soliton dispersion [Eq. (2.21)] changes sign at $h_x^2+2b_1=2\delta$, which means that for $h_x^2+2b_1\gg 2\delta$ the xy soliton is unstable against spontaneous motion.

Thus for $h_x^2+2b_1\ll 2\delta$ the essential contribution to thermodynamical variables comes from the lower branch of the spectrum $E_{xy}(u)$, deviating from the sine-Gordon solution with the increase of the field. For very high fields ($h_x^2+2b_1\gg 2\delta$) the system should behave like a pure sine-Gordon system. For fields near the anisotropic values $h_x^2\simeq 2(\delta-b_1)$ the upper and lower branches in $E_{xy}(u)$ contribute equally. In this limit, therefore, unstable solutions are important in the calculation of thermodynamic variables. We expect then, that we would not observe any form of instability in any measurable parameter in going from $h_x^2+2b_1<2\delta$ to $h_x^2+2b_1>2\delta$. In the next section we will discuss more quantitatively this affirmative in a statistical-mechanics analysis of Hamiltonian (2.1). Following similar steps, we can analyze all other cases. For instance, if $\delta>b_2>b_1+h_x^2/2$, the ground state is along the x direction. Now $\theta=\pi/2$ gives a fully dynamical sine-Gordon soliton in the Φ variables and $\Phi=\pi/2$ gives a static soliton in the θ variable.

Finally, let us consider what happens when $h_z\neq 0$. If

$$b_2<\delta+h_z^2/2, \quad b_2<b_1+h_x^2/2 \ ,$$

the ground state is along the y direction. As we can see, $\Phi=0$ is now only a static solution. We have

$$\Phi=0, \quad \frac{\partial^2\theta}{\partial z^2}=[2(\delta-b_2)+h_z^2]\sin\theta\cos\theta \ . \tag{2.25}$$

The $\Phi=\pi/2$ solution is not changed by the presence of the h_z component. We have a symmetry between the solutions $\Phi=0$ and $\Phi=\pi/2$ just by replacing (δ,h_z) with (b_1,h_x), and so we can use the results obtained before for small velocities [see Eqs. (2.20) and (2.21)]. The other cases can be discussed in a similar way.

Although postponing a thorough discussion of the statistical mechanics of our model until Sec. III, we will calculate here the dynamical correlation function defined as

$$S^{\alpha\alpha}(q,\omega)=\frac{1}{2\pi}\int dt\,dz\,e^{i(qz-\omega t)}\langle S^\alpha(z,t)S^\alpha(0,0)\rangle \ . \tag{2.26}$$

We will be interested (in order to study experimental data) in the fluctuations perpendicular to H_x (i.e., $\alpha=y$).

As we saw above, the soliton model is found to deviate substantially from the sine-Gordon form with a large out-of-plane component when R, defined by Eq. (2.21), is large. Thus, to understand nonlinear effects due to solitons, we need to take into account the out-of-plane fluctuations neglected in the sine-Gordon approximation. Following the approach of Currie *et al.*[19] to evaluate dynamical correlation functions (also, see Ref. 20), we

start with the soliton density n given by

$$n=-\frac{F}{T}=\frac{2}{L}\ln\left[\int\frac{dz\,dp}{2\pi}\exp\{-\beta[E(p)+\Sigma]\}\right], \tag{2.27}$$

where F is the free energy per unit length, L the system size, z the position of the soliton, and $E(p)$ the energy dispersion of soliton. Σ is the "self-energy" of the soliton. Using Eq. (2.22) for small fields and low-velocity solitons, we can write the soliton energy in terms of the linear momentum p. We find

$$E(p)=E_{xy}^0+p^2/2\tilde{m}\ , \tag{2.28}$$

where

$$\tilde{m}=mf(\lambda),\quad m=E_{xy}^0/c^2\ . \tag{2.29}$$

For large λ, $f(\lambda)$ is given by

$$f(\lambda)\simeq 1+8/3\lambda+O(\lambda^{-2})\ . \tag{2.30}$$

Then the out-of-plane component renormalizes the "soliton mass." If we use, for Σ, the result for the pure sine-Gordon model given in Ref. 19, we find, from Eq. (2.27),

$$n=n_{\rm SG}[f(\lambda)]^{1/2}\ , \tag{2.31}$$

where $n_{\rm SG}$ is the usual sine-Gordon result.[19] Using the correct expression for Σ would only change the function $f(\lambda)$ to a new function $g(\lambda)$. In the next section, we will present the correct value for $g(\lambda)$ obtained through the transfer-integral method. The temperature-independent function $g(\lambda)$ is always greater than 1 and approaches 1 as $\lambda\to\infty$.

Within Boltzmann statistics, the probability of finding a soliton with velocity u is

$$P(u)=(\tilde{m}\beta/2\pi)^{1/2}\exp(-\beta\tilde{m}u^2/2)\ . \tag{2.32}$$

The thermal velocity $[u_\theta^2=2\int du\,u^2P(u)]$ being

$$u_\theta=(\beta\tilde{m})^{-1/2}\ . \tag{2.33}$$

The number of solitons plus antisolitons with velocity u is therefore

$$N(u)=2nP(u)\ . \tag{2.34}$$

Using Eq. (2.34), we can calculate Eq. (2.26). For the spin component perpendicular to the direction of the field H_x, we have

$$s_n^y(t)=(-1)^n\cos[\theta_n(t)+(-1)^n v_n(t)]\ . \tag{2.35}$$

In the calculations of correlation functions, we can neglect v_n in Eq. (2.35). To be consistent with the approximation used (i.e., low-velocity solitons), we take for $\theta(t)$ the sine-Gordon result. Following the procedure used by Mikeska[13] for the sine-Gordon model, we obtain (for $\lambda\to\infty$)

$$S^{yy}(q,\omega)=S^2\langle\cos^2\theta\rangle\frac{1}{\pi}\frac{\Gamma_\omega}{\Gamma_\omega^2+\omega^2}\frac{\Gamma_q}{\Gamma_q^2+q^2}\ , \tag{2.36}$$

with $\Gamma_q=4n$ and $\Gamma_\omega=4nu_\theta/\sqrt{\pi}$, and where $\langle\cos^2\theta\rangle=\langle s_y^2\rangle$ will be presented in Sec. III. Using Eqs. (2.31) and (2.33) we obtain

$$\Gamma_q=(\Gamma_q)_{\rm SG}[g(\lambda)]^{1/2},\quad \Gamma_\omega=(\Gamma_\omega)_{\rm SG}[g(\lambda)/f(\lambda)]^{1/2}\ . \tag{2.37}$$

Thus, the effect of the out-of-plane fluctuations at temperatures sufficiently low, such that only low-velocity solitons contribute, is just to renormalize Γ_q and Γ_ω. The functional form $S^{\alpha\alpha}(q,\omega)$ is the same as the one for the sine-Gordon model.[21] This explains why the experimental findings from neutron scattering[21] are qualitatively accounted for by the sine-Gordon theory.

III. STATISTICAL MECHANICS

It has been pointed out by some authors[12,22] that the static properties of the Hamiltonian (2.1) are equivalent to those of a ferromagnetic Heisenberg model with single-site anisotropic terms. To discuss this equivalence in more detail, we start with the partition function, given by the functional integral

$$Z=\int\exp(-\beta\mathscr{H})d\{\cos\theta\}d\{\Phi\}d\{\phi\sin\theta\}d\{v\}\ , \tag{3.1}$$

where $\mathscr{H}$ is given by Eq. (2.3). The functional integral over the components ϕ and v is Gaussian and can therefore be carried out. We obtain

$$Z=Z_{v\phi}Z_{\theta\Phi}\ , \tag{3.2}$$

where $Z_{v\phi}=\text{const}/\beta$ and

$$Z_{\theta\Phi}=\int d\{\cos\theta\}d\{\Phi\}\exp(-\beta\tilde{\mathscr{H}})\ , \tag{3.3}$$

$$\tilde{\mathscr{H}}=JS^2\int\frac{dz}{a}\left[\left[\frac{\partial\theta}{\partial z}\right]^2+\sin^2\theta\left[\frac{\partial\Phi}{\partial z}\right]^2+(2\delta+h_z^2)\right.$$
$$\times\sin^2\theta\cos^2\Phi+(2b_1+h_x^2)\sin^2\theta\sin^2\Phi$$
$$\left.-2h_xh_z\sin^2\theta\sin\Phi\cos\Phi+2b_2\cos^2\theta\right]\ . \tag{3.4}$$

The terms independent of θ and Φ have been omitted in Eq. (3.4). Equation (3.3) is the partition function of an anisotropic Heisenberg ferromagnet,

$$\tilde{\mathscr{H}}=-2J\sum_i\mathbf{S}_i\cdot\mathbf{S}_{i+1}+D\sum_i(S_i^z)^2+B_1\sum_i(S_i^x)^2$$
$$+B_2\sum_i(S_i^y)^2+C\sum S_i^xS_i^z\ , \tag{3.5}$$

with

$$D=2J\delta+Jh_z^2\ , \tag{3.6}$$

$$B_1=2J(b_1-b_2)+Jh_x^2\ , \tag{3.7}$$

$$B_2=2Jb_2\ , \tag{3.8}$$

$$C=2Jh_xh_z\ . \tag{3.9}$$

Using the condition

$$(S_i^x)^2+(S_i^y)^2+(S_i^z)^2=S^2\ , \tag{3.10}$$

we can eliminate one of the components $(S_i^\alpha)^2$ (α is chosen such that the final anisotropic parameters are positive) and write Hamiltonian (3.5) in terms of two anisotropies and a crossed term. There will be an extra term independent of spin operators, which we will neglect.

If one of the field components H_x or H_z is zero (then C vanishes), the magnetic field is equivalent to an effective anisotropy given by Eq. (3.6) or (3.7).

The thermodynamic properties are studied through thermal averages of operators given by

$$\langle F\rangle=\frac{1}{Z}\int d\{\cos\theta\}d\{\Phi\}d\{\phi\sin\theta\}d\{v\}Fe^{-\beta\mathscr{H}} . \quad (3.11)$$

If F depends only on θ and Φ, then the integrals in v and ϕ can be derived as before and we obtain

$$\langle F\rangle=\frac{1}{Z_{v\phi}}\int d\{\cos\theta\}d\{\Phi\}Fe^{-\beta\tilde{\mathscr{H}}} . \quad (3.12)$$

Then the equivalence between the Hamiltonians (2.1) and (3.5) can be correctly expressed as the thermodynamical properties of Hamiltonian (2.1), for operators depending only on the variables θ and Φ are the same as those of the Hamiltonian (3.5). In the calculation of variables such as susceptibilities and correlation length, we can neglect the small quantities v and ϕ in the expressions for the corresponding operators in the integrand of (3.11) and then obtain the same results using Hamiltonian (2.1) or (3.5).

The statistical mechanics of the classical Hamiltonian (3.5) can be studied by means of the transfer-integral method.[23] The easy axis for the spin system will result from the competition between the anisotropic terms. Different cases have to be considered. Let us start, for simplicity, with the following cases:

(i) $b_2=0$ [otherwise we could use Eq. (3.10) to eliminate $(S_i^y)^2$]. The easy axis for the spin system corresponds to the y axis. In the case of low temperatures ($T\ll JS^2$) and weak anisotropies ($D, B_1\ll J$), the problem is reduced to solving the equation[3]

$$\left[-\frac{1}{2\tilde{m}}\nabla_s^2+\frac{p}{2}s_x^2+\tfrac{1}{2}s_z^2+\tfrac{1}{2}rs_xs_z\right]\psi_n(\mathbf{s})=\tilde{\epsilon}_n\psi_n(\mathbf{s}) , \quad (3.13)$$

where

$$\sqrt{\tilde{m}}\equiv 2S^2\sqrt{JD}\,/T,\quad p\equiv B_1/D,\quad r=C/D , \quad (3.14)$$

$$\nabla_s^2=\frac{\partial^2}{\partial s_x^2}+\frac{\partial^2}{\partial s_y^2}+\frac{\partial^2}{\partial s_z^2},\quad s_x^2+s_y^2+s_z^2=1 . \quad (3.15)$$

Now we can make a rotation in the s_x,s_z plane to diagonalize Eq. (3.13). We find

$$\left[-\frac{1}{2m^*}\nabla_{s'}^2+\frac{\Delta}{2}s_{x'}^2+\tfrac{1}{2}s_{z'}^2\right]\psi_n(\mathbf{s})=\epsilon_n\psi_n(\mathbf{s}) , \quad (3.16)$$

where

$$m^*=\lambda_-\tilde{m},\quad \Delta=\lambda_+/\lambda_-,\quad \epsilon_n=\tilde{\epsilon}/\lambda_- , \quad (3.17)$$

and

$$\lambda_\pm=0.5\{(p+1)\pm[(p-1)^2+r^2]^{1/2}\} . \quad (3.18)$$

Let

$$A=T^2m^*(4JS^4)^{-1}=\lambda_-D , \quad (3.19)$$

$$B=\Delta A=\lambda_+D . \quad (3.20)$$

We see that if $r=0$, we have $A=D$ and $B=B_1$.

Equation (3.16), with $A\geq B$, has been solved by Sasaki[3] and thus, using his results we can calculate the susceptibilities, inverse correlation lengths, static correlation functions, etc., for Hamiltonian (2.1). From now on, we will take $h_z=0$; then in all statistical mechanics calculations (with $b_2=0$), the total anisotropy in the x direction can be defined through an effective anisotropic field along the x axis given by

$$h_{\text{eff}}^x=(2b_1+h_x^2)^{1/2} . \quad (3.21)$$

$A\geq B$ means $h_{\text{eff}}^x\leq\sqrt{2\delta}$. If $h_{\text{eff}}^x=\sqrt{2\delta}$, Hamiltonian (3.5) is equivalent to the one solved exactly by Faria and Pires.[24]

(ii) $b_1=0$ and $b_2>h_x^2/2$. We will always take $b_2<\delta$; then, $h_x<\sqrt{2\delta}$. Using Eq. (3.10) to eliminate $(S_i^x)^2$, Eq. (3.5) can be written as

$$\mathscr{H}=-2J\sum_i\mathbf{S}_i\cdot\mathbf{S}_{i+1}+A\sum_i(S_i^z)^2+B\sum_i(S_i^y)^2 , \quad (3.22)$$

with

$$A=2J(\delta-h_x^2/2),\quad B=2J(b_2-h_x^2/2) . \quad (3.23)$$

The effective field is now given by

$$\begin{aligned}&h_{\text{eff}}^z=(2\delta-h_x^2)^{1/2} ,\\ &h_{\text{eff}}^y=(2b_2-h_x^2)^{1/2}\quad (b_2^2>h^2/2) .\end{aligned} \quad (3.24)$$

h_{eff} decreases with increasing h_x. The easy direction is along the x axis.

(iii) $b_1=0$ and $h_x^2>2b_2$. Using Eq. (3.10) to eliminate $(S_i^y)^2$, Eq. (3.5) can be written as

$$\mathscr{H}=-2J\sum_i\mathbf{S}_i\cdot\mathbf{S}_{i+1}+A\sum_i(S_i^z)^2+B\sum_i(S_i^x)^2 , \quad (3.25)$$

with

$$A=2J(\delta-b_2),\quad B=2J(h_x^2/2-b_2) . \quad (3.26)$$

The effective field is

$$h_{\text{eff}}^x=(h_x^2-2b_2)^{1/2} , \quad (3.27)$$

and we have an effective anisotropy in the z axis,

$$\delta_{\text{eff}}=\delta-b_2 . \quad (3.28)$$

The easy axis corresponds to the y axis. If $h_x^2=2b_2$, as a consequence $h_{\text{eff}}^x=0$ and the system is equivalent to a model with no external field but with an effective anisotropy in the z axis. The isotropic character in the xy plane is restored.

With the aim of using our calculation in the next section to analyze experimental data in TMMC, we will now discuss in more detail the case $b_1=b_2=0$, $H_z=0$. Using the equations given by Sasaki[3] and solving them numerically, we could obtain results for any values of the parameters A and B (this is δ and h_x). However, we will use an asymptotic expansion given in the same reference that, in fact, for low temperatures, covers most of the region of

interest. In the following, two energies will be important: the soliton energy associated with the magnetic field $E_h=4S^2\sqrt{JB}=4JS^2h$ and the energy associated with the anisotropy $E_d=4S^2\sqrt{JA}=4JS^2\sqrt{2\delta}$. To understand what happens to the ferromagnet, we should consider several relations between the parameters (let $B\leq A$; if $h^2\geq 2\delta$, we just change B for A). Since we are concerned with low temperatures, we should have $T\ll E_d$.

If $h^2\ll 2\delta(\Delta\ll 1)$, the spins are confined to the vicinity of the xy plane. If $T\gg E_h$, only spin waves contribute to the thermodynamics. If $T\ll E_h$, the soliton contribution will be important. We note that for large T, the system behaves like an XY model. For small T, the spins are aligned almost parallel (or antiparallel) to the y axis. We say that the system is in the "Ising region," although in the soliton, the spins turn in the xy plane because $h^2\ll 2\delta$. Since some authors call this region xy-like, we call it XY_{Ising}.

If $h^2=2\delta$, we have a classical Ising model. For $h^2\sim 2\delta$ the system should behave like a true Ising model with the spins turning in any plane in going from z to $-z$. However, for the solitons to be important we should have $T\ll E_d$, but now $E_d\sim E_h$ and so $T\ll E_h$. Thus the condition for the Ising region is always $T\ll E_h$.

One of the most important variables in the analysis of experimental data is the inverse correlation length K_y for the spin component in the xy plane perpendicular to the direction of the applied magnetic field. As we saw in Sec. II, K_y directly gives the soliton density. For the XY region ($\Delta\ll 1$) we have[3]

$$K_y=T[a_1(q)-a_0(q)]^{-1}/4JS^2\ , \tag{3.29}$$

where

$$|q|=JS^4B/T^2=(JS^2h/T)^2\ , \tag{3.30}$$

and $a_n(q)$ are the characteristic values of the Mathieu equation.[25] We can use Eq. (3.29) in the whole XY region. For $|q|\ll 1$ (i.e., $T\gg E_h$) we have[25]

$$K_y=\frac{T}{4JS^2}\left[1+q+\tfrac{3}{8}q^2-q^3/64-\tfrac{85}{1536}q^4+\tfrac{11}{36\,864}q^5+\cdots\right]^{-1}\ , \tag{3.31}$$

where the first three terms give the spin-wave results.

For $|q|\gg 1$ (i.e., $T\ll E_h$), we obtain[3]

$$K_y=8\left[\frac{2}{\pi}\right]^{1/2}J^{1/2}Sh\left[\frac{h}{T}\right]^{1/2}e^{-4JS^2h/T}\ , \tag{3.32}$$

in the XY_{Ising} region. Equation (3.32) is the well-known result for the pure sine-Gordon chain.[19]

For the Ising region (including the pure Ising and the XY_{Ising}), $T\ll E_h$ and we have[3]

$$K_y=4DS^2\tau_0/T\ , \tag{3.33}$$

where

$$\tau_0=4\sqrt{2}\Delta^{3/4}(1+\sqrt{\Delta})^{1/2}e^{-E_h/T}e^{-\zeta}I_0(\zeta)\ , \tag{3.34}$$

$$\zeta=[(1-\sqrt{\Delta})/2\sqrt{\Delta}](E_h/T)\ , \tag{3.35}$$

and as before, $D=2J\delta$. I_0 is the modified Bessel function. Equation (3.33) can be explicitly written as ($B\leq A$)

$$K_y=\frac{K_p}{T^{1/2}}\left[\frac{h}{T}\right]^{3/2}64\sqrt{2}J^2S^4(2\delta)^{1/4}\times\left[1+\frac{h}{\sqrt{2\delta}}\right]^{1/2}e^{-\beta E_h}e^{-\zeta}I_0(\zeta)\ , \tag{3.36}$$

where $K_p=T/4JS^2$ is the inverse correlation length for the planar model. For $A=B$ (i.e., $h=\sqrt{2\delta}$), Eq. (3.36) is identical to the result of Nakamura and Sasada for the pure Ising chain:[26]

$$K_y=\frac{32JS^2h^2}{T}e^{-4JS^2h/T}\ . \tag{3.37}$$

In the $(XY)_{\text{Ising}}$ region, ζ is very large and we can use the expansion for $I_0(\zeta)$ for large ζ, obtaining

$$K_y=(K_y)_{\text{SG}}\left[\frac{1+h/\sqrt{2\delta}}{1-h/\sqrt{2\delta}}\right]^{1/2}\ , \tag{3.38}$$

where $(K_y)_{\text{SG}}$ is the inverse correlation length for the pure sine-Gordon chain given by Eq. (3.32). Equation (3.38) is valid if $\zeta\gg\frac{1}{8}$.

In order to make a comparison with experimental data,[27–32] in the next section, we will define an energy E_s and a parameter α by

$$E_s=-T\ln\left[\left[\frac{\pi}{2}\right]^{1/2}\frac{JS^2T^{1/2}}{(\gamma HS)^{3/2}}K_y\right] \tag{3.39}$$

and

$$\alpha=\frac{\partial\ln}{\partial u}\left[\frac{K_y}{K_p}\left[\frac{T}{H}\right]^{3/2}\right]\ , \tag{3.40}$$

with $u=H/T$, and here we will use H and D instead of h and δ. For the sine-Gordon model, E_s is just E_h and $\alpha=\alpha_{\text{SG}}=\gamma S$ is the constant relating the field to the energy E_h ($=\alpha H$).

Using Eq. (3.36), we obtain

$$E_s=-T\ln[2\sqrt{\pi}S(JD)^{1/4}R(u,T)e^{-\beta E_n}]\ , \tag{3.41}$$

where

$$R(u,T)=(1/T+\gamma u/4S\sqrt{JD}\,)^{1/2}e^{-\zeta}I_0(\zeta) \tag{3.42}$$

and

$$\alpha=\alpha_{\text{SG}}-\alpha_{\text{OP}}\ , \tag{3.43}$$

where

$$\alpha_{\text{OP}}=\frac{\partial\ln}{\partial u}R(u,T)\ , \tag{3.44}$$

is the correction to α_{SG} due to fluctuations out of the xy plane. In the $(XY)_{\text{Ising}}$ region we can use the expansion for $I_0(\zeta)$ for large ζ, obtaining

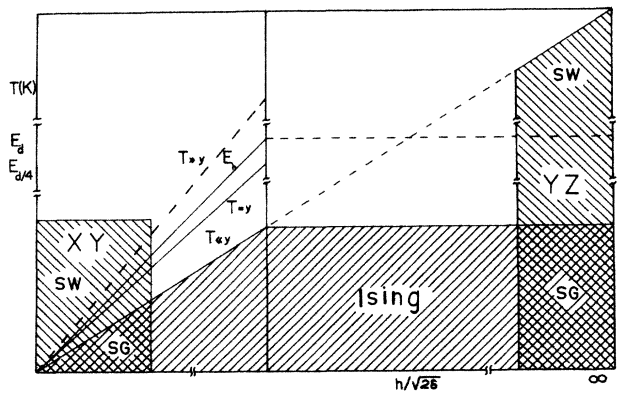

FIG. 1. A rough sketch of the regions discussed in Sec. III. The dashed areas indicate the XY, the YZ, the Ising, and their intersections, the XY_{Ising} and YZ_{Ising} regions. The XY region is given by $h \ll \sqrt{2}\delta$, $T \ll E_d/4$ ($E_d = 4JS^2\sqrt{2}\delta$). In this region, we have the spin-wave (SW) limit $|q| \ll 1$ ($T \gg y$, where $y = JS^2h$) and the sine-Gordon (SG) limit $|q| \gg 1$ ($T \ll y$). The YZ region is given by $h \gg \sqrt{2}\delta$, $T \ll y$. In this region, the SW limit is $T \gg E_d/4$ and the SG limit is $T \ll E_d/4$. The Ising region is given by $T \ll E_h$ ($E_h = 4y$) for $h \lesssim \sqrt{2}\delta$, and $T \ll E_d$ for $h \gtrsim \sqrt{2}\delta$. The parameter δ is kept constant while T and h are varied.

$$\alpha_{\text{OP}} \simeq \alpha_{\text{SG}} \left[4\sqrt{JD}\,\frac{T}{16JS^2D - \gamma^2H^2} + \frac{T^2}{4S(4S\sqrt{DJ} - L_0\gamma H)^2} \right] . \tag{3.45}$$

For $\Delta \sim 1$ ($A \sim B$), $\zeta \simeq 0$, and we can take $I_0(\zeta) \simeq 1$. We obtain

$$\alpha = \frac{\alpha_{\text{SG}}}{2} \left[1 - \frac{T}{4S\sqrt{JD} + \gamma H} \right] . \tag{3.46}$$

The results of this section can be best analyzed through Fig. 1, where we show the XY, the YZ, the Ising and their intersection, the $(XY)_{\text{Ising}}$, and $(YZ)_{\text{Ising}}$ regions. The XY region is given by $h \ll \sqrt{2}\delta$, $T \ll JS^2\sqrt{2}\delta$. In this region, we have the spin-wave (SW) limit $|q| \ll 1$ and the sine-Gordon (SG) limit $|q| \gg 1$. The YZ region is given by $h \gg \sqrt{2}\delta$, $T \ll JS^2h$. In this region, the SW limit is $T \gg JS^2\sqrt{2}\delta$ and the SG limit is $T \ll JS^2\sqrt{2}\delta$. The Ising region is given by $T \ll E_h$ for $h \lesssim \sqrt{2}\delta$ and $T \ll E_d$ for $h \gtrsim \sqrt{2}\delta$. For $h \lesssim \sqrt{2}\delta$, Eq. (3.29) is valid in the XY region, as is Eq. (3.36) in the Ising region. Equation (3.38) is a correction to the SG expression and Eq. (3.31) is an asymptotic expansion in the SW limit. All these equations can be used for $h \gtrsim \sqrt{2}\delta$ by just changing h for $\sqrt{2}\delta$ and vice versa.

IV. APPLICATION TO TMMC [$(CD_3)_4NMnCl_3$]

At room temperature, the crystal structure of TMMC is hexagonal. At $T \simeq 126$ K, the tetramethyl ammonium ions undergo an order-disorder transition and the structure becomes monoclinic.[27] The magnetic properties of TMMC are not strongly affected by the structural behavior, in that the $MnCl_3$ chains are not appreciably distorted when the temperature is lowered. However, a small magnetic anisotropy b is induced within the XY plane (easy plane) perpendicular to the chain axis.[18] However, because of the structural phase transition, three crystallographic domains coexist in a single crystal of TMMC, below 126 K. For each domain, the orientation of the effective field, describing the anisotropy, is different, resulting in different values of the total effective field being actually experienced by the electron spin.[27]

To allow several orientations of the anisotropic axis in relation to the external field H, let us suppose that H is in the x direction but the anisotropy is in the η direction making an angle θ with the x axis. The z component is not changed. Then we have

$$S_\eta^2 = S_x^2\cos^2\theta + S_y^2\sin^2\theta + 2S_xS_y\cos\theta\sin\theta . \tag{4.1}$$

Taking an average over θ, we obtain

$$S_\eta^2 = \tfrac{1}{2}S_x^2 + \tfrac{1}{2}S_y^2 . \tag{4.2}$$

Thus, if the anisotropic term is bS_η^2, we have for the equivalent ferromagnet

$$\mathcal{H} = -2J\sum_i \mathbf{S}_i\cdot\mathbf{S}_{i+1} + 2J\delta\sum_i (S_i^z)^2 + Jb\sum_i (S_i^y)^2 + J(b+h^2)\sum_i (S_i^x)^2 . \tag{4.3}$$

Using Eq. (3.10) to eliminate $(S_i^y)^2$, we obtain

$$\mathcal{H} = -2J\sum_i \mathbf{S}_i\cdot\mathbf{S}_{i+1} + A\sum_i (S_i^z)^2 + B\sum_i (S_i^x)^2 , \tag{4.4}$$

with

$$A = 2J(\delta - b/2), \quad B = Jh^2 .$$

Thus, in a configurational average, the effect of b is to renormalize the parameter δ.

The δ value calculated for TMMC on the basis of a full Ewald sum for the classical magnetic dipole-dipole coupling alone[33] is $\delta = 0.014$. However, δ obtained from the measured energy gap in the spin-wave spectrum[33] is $\delta = 0.0086$. Boucher[34] and Pires and Gouvea,[35] analyzing low-temperature EPR shift, have obtained $\delta = 0.0123$ and 0.0101, respectively, in agreement with the results of Heilmann *et al.*[31] The discrepancy between the classical value and the experimental one has been attributed to single-ion anisotropy effects as well as quantum corrections.[31] In this paper, we use the value $\delta = 0.0101$ (which corresponds to an effective field of $H_d = 69$ kOe) obtained from Ref. 35. For J, we take the usual value $J = 6.5$ K.

In Fig. 2 we plot K_y as a function of the external field in the x direction for fixed T. We have used Eqs. (3.29) and (3.33) to calculate K_y and as we can see, K_y decreases during the XY_- Ising crossover transition and very large effects can be expected,[27] even for relatively small values of H.

In Fig. 3 we present $K_y[H(H/T)^{1/2}]^{-1}$ as a function of H/T for $T = 2.5$ K on a semilog scale. The experimental

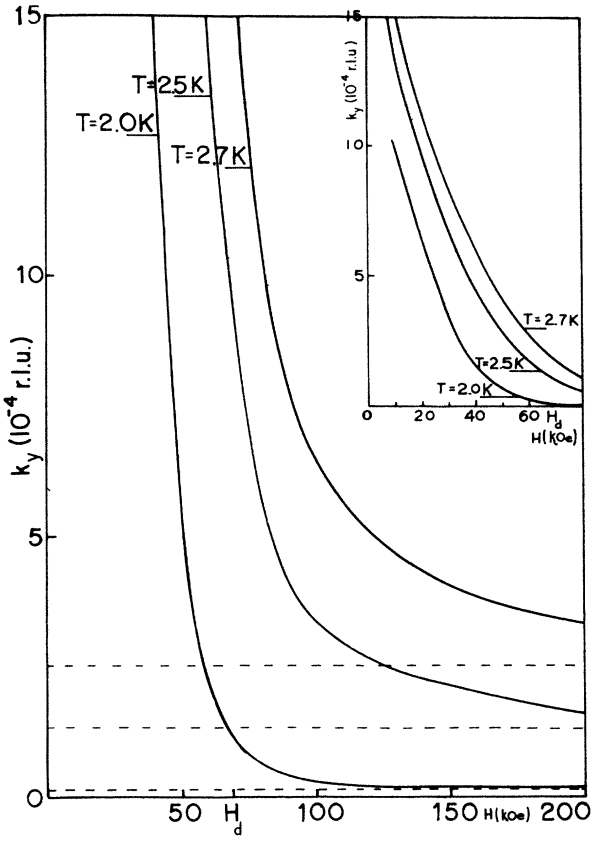

FIG. 2. Inverse correlation length K_y as a function of the magnetic H for different temperatures.

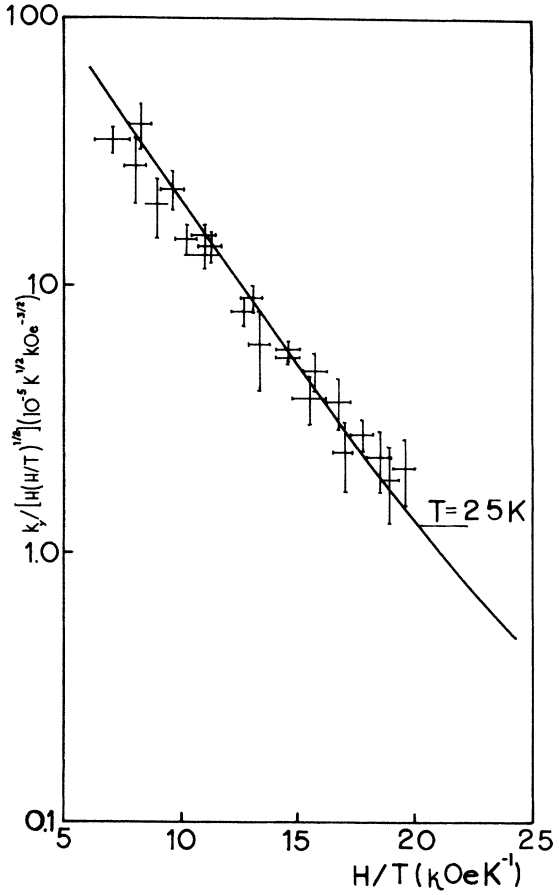

FIG. 3. Comparison between theory (solid lines) and experimental data from Ref. 25, for K_y as a function of H/T. (K_y is given in reciprocal lattice units.)

data is from Ref. 25. As we can see, the agreement is very good.

The energy parameter α can be calculated directly from Eqs. (3.43) and (3.44). For instance, for $T=2.5$ K, $H=36$ kOe (as in Ref. 25), we have $\Delta=0.28$, $E_h=12.16$ K. Since for these values $T \ll E_h$, $\Delta<1$, we can use Eqs. (3.43) and (3.45), obtaining $\alpha=0.28$ K/kOe in close agreement with the experimental value[28] $\alpha=0.26\pm0.03$ K/kOe. Figure 4 shows α as a function of H/T for various temperatures. As we can see, for very low temperatures α is approximately constant for $10<H/T<25$, in agreement with Fig. 3 and experimental results.

From Eq. (3.33) and the discussion about the dynamics in Sec. II, we expect that for high magnetic fields in the x direction (i.e., $H \gg H_d$) the system should behave like a sine-Gordon model in the yz plane with energy $E_d=4JS^2\sqrt{2\delta}=23.1$ K independent of the value of the applied field. In this limit, we have from Eq. (3.33),

$$K_y=8\left[\frac{2}{\pi}\right]^{1/2}\frac{SJ^{1/2}}{T^{1/2}}(2\delta)^{3/4}\exp\left[-\frac{4JS^2\sqrt{2\delta}}{T}\right], \quad (4.5)$$

where for $H>H_d$ we have exchanged h for $\sqrt{2\delta}$ and vice versa. In a similar way, as we did for low fields, we define a function G by

$$G=T^{3/2}K_y/K_p\ , \quad (4.6)$$

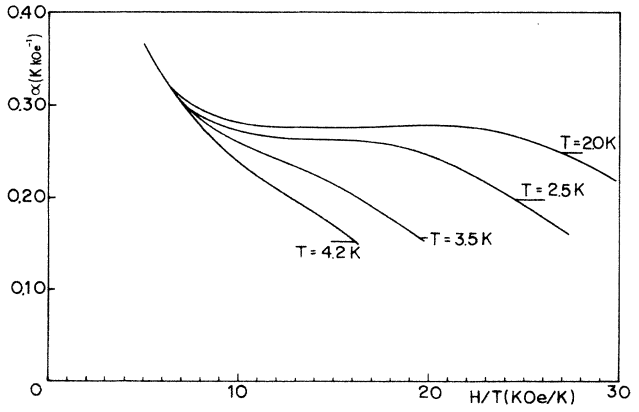

FIG. 4. Parameter α defined by Eq. (3.40) as a function of H/T for various temperatures.

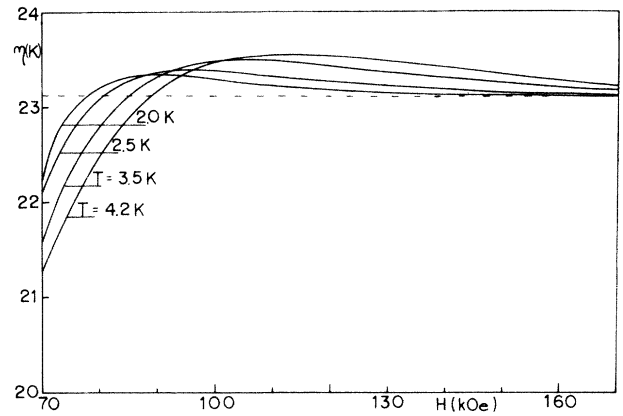

FIG. 5. Parameter η defined by Eq. (4.7) as a function of the magnetic field H for various temperatures. The dashed line is the sine-Gordon value $\eta=23.13$ K.

and the equivalent to the α parameter by

$$\eta=-\frac{\partial \ln G}{\partial \beta} . \tag{4.7}$$

In the sine-Gordon limit $\eta=4JS^2\sqrt{2\delta}=E_d$, as it should. In Fig. 5 we show η as a function of H for some values of the temperature. For H just above H_d (i.e., $h=\sqrt{2\delta}$), η depends strongly on H, but for larger fields, η tends to the sine-Gordon value. The crossover from the xy soliton to the yz soliton can be seen best in Fig. 6, where we show

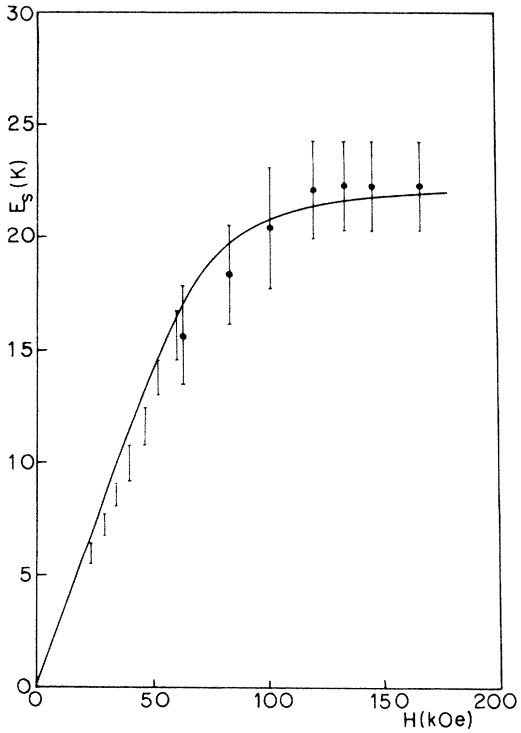

FIG. 6. Soliton energy as a function of the magnetic field. The solid line is calculated theoretically for a temperature $T=2.4$ K. The experimental data are from Ref. 32.

the soliton energy, calculated from Eq. (3.39), as a function of H, for $T=2.4$ K. The experimental data are from Ref. 32. As we can see, the agreement between theory and experiment is very good. Thus, for $T\ll 23$ K and $H\gg 70$ kOe the system should behave like a pure SG model, the SG behavior being so much more apparent at large fields ($h\gg\sqrt{2\delta}$) than at small fields ($h\ll\sqrt{2\delta}$).

To complete our study of neutron scattering data, we will consider the maximum of the intensity integrated over energy of the central peak at $q=0$. As pointed out by Regnault *et al.*,[29] the pure sine-Gordon soliton model fails to explain the data of the intensity integrated over ω, for $T=2.5$ K and $H\lesssim 30$ kOe. The contribution from $S_{||}(q,\omega)$ is diverging (see Ref. 27). This behavior is clearly unphysical and indicates the limits of field and temperature within which the pure sine-Gordon model is applicable. In the limit of small H and T, Regnault *et al.*[29] have used a perturbation expansion in H/T to fit the experimental data. Here we use a single theory which gives correct results in both limits. At low temperature, the scattering intensity integrated over energy is given by[29]

$$S(q)=\frac{S^2}{\pi}\left[\langle s_x^2\rangle\frac{K_x}{K_x^2+q^2}+\langle s_y^2\rangle\frac{K_y}{K_y^2+q^2}\cos\beta\right], \tag{4.8}$$

where β is the angle between the scattering vector $\mathbf{Q}_0$ and the chain axis. In the Ising region ($T\ll E_h$), K_y is given by Eq. (3.33). The other variables are given by[3]

$$K_x=h_x,\quad \langle s_x^2\rangle=T(4Jh_x)^{-1}, \tag{4.9a}$$

$$\langle s_y^2\rangle=\left[1-\frac{T}{4J}\left[\frac{1}{\sqrt{2\delta}}+\frac{1}{h_x}\right]\right] . \tag{4.9b}$$

In the XY region ($h\ll\sqrt{2\delta}$), K_y is given by Eq. (3.29) and K_x is[3]

$$K_x=T[b_1(q)-a_0(q)]^{-1}/4JS^2 , \tag{4.10}$$

where $b_1(q)$ and $a_0(q)$ are characteristic values of the Mathieu equation[25] and q was defined in Eq. (3.30). Because $\langle s_x^2\rangle$ and $\langle s_y^2\rangle$ are not given explicitly in Ref. 3, they are calculated in the Appendix.

The convoluted intensity $I(\mathbf{Q}_0,q)$ to be compared with the experimental data is obtained from Eq. (4.8) using the procedure of Ref. 29. In Fig. 7 we show $I(\mathbf{Q}_0,0)$ as a function of the external magnetic field for $T=2.5$ K. The solid curve was calculated using the equations for the Ising region, the dashed curve using the equations for the XY region.

To complete our study of TMMC we will calculate the three-dimensional ordering temperature T_N as a function of the magnetic field. This calculation has already been done by Boucher[17] using the sine-Gordon model and ascribing the deviation of his theory from the experimental $T_N(H)$ to an impurity effect. Later, Harada *et al.*,[12] using numerical calculation, obtained good agreement with experiments for $H>30$ kOe. In the simplest description where the interchain coupling J' is treated in the mean-field approximation, we have T_N given by $J'\chi_\pi^\alpha(T_N)\simeq 1$, where $\chi_\pi^\alpha(T)$ is the 1D staggered susceptibility measured in the direction α of the easy-magnetization axis. In the presence of a magnetic field, we have

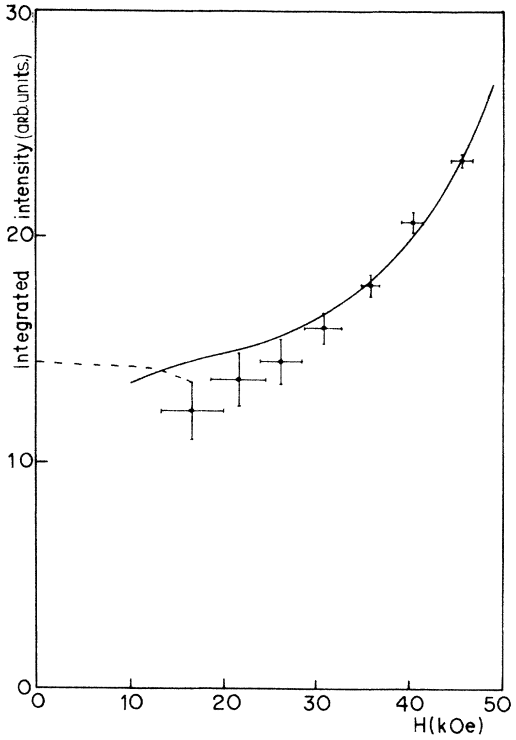

FIG. 7. Maximum of the intensity integrated over energy of the central peak (at $q=0$) as a function of the magnetic field for $T=2.5$ K. Solid line, calculation for the Ising region; dashed line, XY region. The experimental data are from Ref. 29.

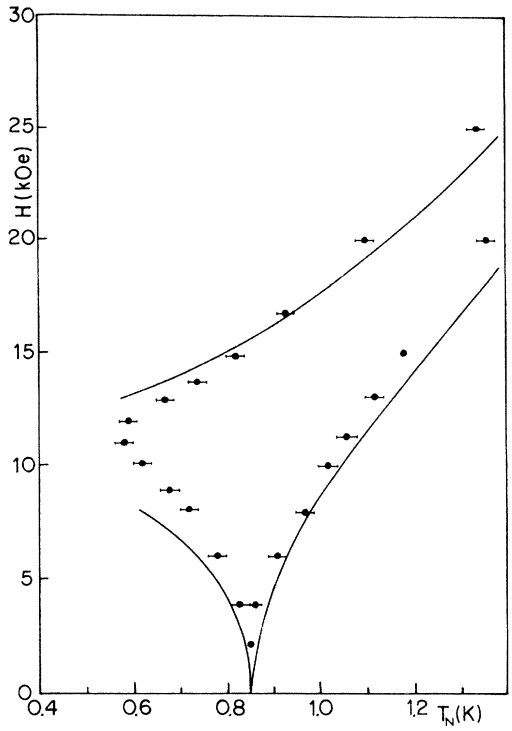

FIG. 9. Phase diagram of TMMC for H perpendicular to the chain axis. The experimental data are from Ref. 17.

$$\chi_\pi^\alpha(T_N(H))=\chi_\pi^{\alpha'}(T_N(H=0)) ,$$

with α and α' possibly different. The resulting curve for $T_N(H)$, with experimental data from Ref. 21, is shown in Fig. 8. In Fig. 9 we show the phase diagram of TMMC. The experimental data are from Ref. 17. This diagram can be interpreted by taking into account the small anisotropy b in the plane perpendicular to the chain.[17,18] Boucher[17] calculated parts of the diagram using perturbation expansion and numerical results obtained by Loveluck.[36] Our calculations were done using only one theory. For a better discussion of this diagram, the reader should refer to Refs. 17 and 18.

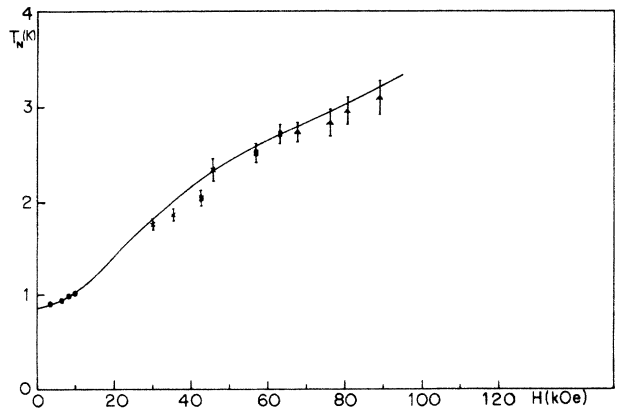

FIG. 8. Field dependence of the three-dimensional ordering temperature. The experimental data are from Ref. 17.

It should be interesting to have experiments done with the applied field, making an angle θ with the chain direction (i.e., keeping H constant but varying θ). Using Eqs. (3.19) and (3.20) and taking

$$H_z=H\cos\theta, \quad H_x=H\sin\theta , \tag{4.11}$$

we have, explicitly,

$$\begin{aligned} A&=0.5J\{(2\delta+h^2)-[(2\delta+h^2)^2-8\delta h^2\sin^2\theta]^{1/2}\} , \\ B&=0.5J\{(2\delta+h^2)+[(2\delta+h^2)^2-8\delta h^2\sin^2\theta]^{1/2}\} . \end{aligned} \tag{4.12}$$

Inserting Eq. (4.12) into Eq. (3.33), we can calculate K_y as a function of θ, and compare it with experimental data, should it become available.

V. CONCLUSION

In this paper we have studied the dynamic and thermodynamic properties of a classical one-dimensional anisotropic antiferromagnet in the presence of an external magnetic field. Our results were based on the classical continuum limit. We have neglected quantum effects which have been discussed by Maki,[37] Mikeska,[38] and Riseborough,[39] and discreteness effects which have been investigated by Riseborough *et al.*[40] Using Mikeska's calculations,[38] the quantum correction to the soliton energy is

$$E_s(\text{quantum}) = E_s^0(\text{classical})[\sqrt{S(S+1)} - \tfrac{1}{2}]/S \ ,$$

which, for $S = \frac{5}{2}$, gives $E_s(\text{quantum}) = 0.98 E_s^0(\text{classical})$, a negligible correction. However, we think that quantum corrections have already been taken into account in the use of the value of δ obtained from fitting experimental data instead of the classical value. The discreteness effect seems to play no role at the temperatures of our calculations.[40]

To conclude, we can say that within the experimental accuracy, and since there are no adjustable parameters, the agreement between our theory and experiments may be considered very good.

ACKNOWLEDGMENTS

This work was started while one of the authors (A.P.) was at Département de Recherche Fondamentale, Centre d'Etudes Nucléaires de Grenoble. Helpful discussions with Dr. Boucher are gratefully acknowledged. We are grateful to Centre National de la Recherche Scientifique (France), Conselho Nacional de Desenvolvimento Cientifico e Technologico (Brazil), and Financiadora de Estudos e Projetos (Brazil) for financial support.

APPENDIX

Following the procedure given in Ref. 3, we have

$$\langle s_x^2 \rangle = |\langle \psi_x | S_x | \psi_0 \rangle|^2 \quad \text{and} \quad \langle s_y^2 \rangle = |\langle \psi_y | S_y | \psi_0 \rangle|^2 \ ,$$

where

$$\psi_0 = N_0 \mathrm{ce}_0(\theta,q)\exp[-(m^*)^{1/2}v^2/2] \ ,$$

$$\psi_x = N_x \mathrm{se}_1(\theta,q)\exp[-(m^*)^{1/2}v^2/2] \ ,$$

and

$$\psi_y = N_y \mathrm{ce}_1(\theta,q)\exp[-(m^*)^{1/2}v^2/2] \ .$$

In the above expressions, θ and v are coordinates defined in Ref. 3, $\mathrm{ce}_0(\theta,q)$, $\mathrm{ce}_1(\theta,q)$, and $\mathrm{se}_1(\theta,q)$ are the Mathieu functions,[25] and N_α ($\alpha = 0,x,y$) are normalization constants determined by imposing the condition $|\langle \psi_\alpha | \psi_\alpha \rangle| = 1$. The parameter m^* is given by Eq. (3.17).

Explicitly, $\langle s_x^2 \rangle$ and $\langle s_y^2 \rangle$ are obtained by solving the integrals

$$\langle \psi_x | S_x | \psi_0 \rangle = N_0 N_x \int_{-\infty}^{+\infty} (\mathrm{sech}v)\exp[-(m^*)^{1/2}v^2]dv \int_0^{\pi} \sin\theta \, \mathrm{ce}_0(\theta)\mathrm{se}_1(\theta) f(v,\theta) d\theta$$

and

$$\langle \psi_y | S_y | \psi_0 \rangle = N_0 N_y \int_{-\infty}^{\infty} [1-(1-\Delta)\tanh^2 v]^{1/2}\exp[-(m^*)^{1/2}v^2]dv \int_0^{\pi} \cos\theta \, \mathrm{ce}_0(\theta)\mathrm{ce}_1(\theta) f(v,\theta) d\theta \ ,$$

where

$$f(v,\theta) = (\mathrm{sech}v)\left| \frac{[1-(1-\Delta)\tanh^2 v]^{1/2}}{[1-\Delta\cos^2\theta]^{1/2}} - \frac{\Delta\cos^2\theta}{[1-(1-\Delta)\tanh^2 v]^{1/2}[1-\Delta\cos^2\theta]^{1/2}} \right|$$

is the Jacobian related to the transformation of coordinates done in Ref. 3.

[1] J. Bernasconi and T. Schneider, *Physics in One Dimension* (Springer, Berlin, 1980).
[2] H. J. Mikeska, J. Phys. C **11**, L29 (1978).
[3] K. Sasaki, Prog. Theor. Phys. **68**, 1518 (1982).
[4] C. Etrich and H. J. Mikeska, J. Phys. C **16**, 4889 (1983).
[5] H. C. Fogedby, P. Hedegard, and A. Svane, J. Phys. C **17**, 3475 (1984).
[6] H. J. Mikeska and K. Osano, Z. Phys. B **52**, 111 (1983).
[7] H. J. Mikeska, J. Appl. Phys. **52**, 1950 (1981).
[8] E. Magyari and H. Thomas, Phys. Rev. B **25**, 531 (1982).
[9] P. Kumar, Phys. Rev. B **25**, 483 (1982).
[10] H. J. Mikeska, *Physics in One Dimension*, Ref. 1, p. 153.
[11] K. Osano, J. Phys. C **17**, 843 (1984).
[12] I. Harada, K. Sasaki, and H. Shiba, Solid State Commun. **40**, 29 (1981).
[13] H. J. Mikeska, J. Phys. C **13**, 2913 (1980).
[14] N. Flüggen and H. J. Mikeska, Solid State Commun. **48**, 293 (1983).
[15] K. M. Leung, D. W. Hone, D. L. Mills, P. S. Riseborough, and S. E. Trullinger, Phys. Rev. B **21**, 4017 (1980).
[16] D. Hone and A. S. T. Pires, Phys. Rev. B **15**, 323 (1977).
[17] J. P. Boucher, Solid State Commun. **33**, 1025 (1980).
[18] K. Takeda, T. Koide, T. Tonegawa, and I. Harada, J. Phys. Soc. Jpn. **48**, 1115 (1980).
[19] J. F. Currie, J. A. Krumhansl, A. R. Bishop, and S. E. Trullinger, Phys. Rev. B **22**, 477 (1980).
[20] K. Osano, J. Phys. C **17**, L511 (1984).
[21] J. P. Boucher, L. P. Regnault, J. Rossat-Mignod, J. P. Renard, J. Bouillot, and W. G. Stirling, J. Appl. Phys. **52**, 1956 (1981).
[22] J. Villain and J. M. Loveluck, J. Phys. (Paris) Lett. **38**, L77 (1977).
[23] D. J. Scalapino, M. Sears, and R. A. Ferrel, Phys. Rev. B **6**, 3409 (1972).
[24] A. C. Faria and A. S. T. Pires, J. Phys. C **12**, 2637 (1979).
[25] M. Abramowitz and I. A. Stegun, *Handbook of Mathematical Functions* (Dover, New York, 1970).
[26] K. Nakamura and T. Sasada, J. Phys. C **11**, 331 (1978).
[27] J. P. Boucher, L. P. Regnault, J. Rossat-Mignod, J. Villain, and J. P. Renard, Solid State Commun. **31**, 311 (1979).
[28] J. P. Boucher, L. P. Regnault, J. Rossat-Mignod, J. P. Renard, J. Bouillot, and W. G. Stirling, Solid State Commun. **33**, 171 (1980).
[29] L. P. Regnault, J. P. Boucher, J. Rossat-Mignod, J. P. Renard, J. Bouillot, and W. G. Stirling, J. Phys. C **15**, 1261 (1982).
[30] J. P. Boucher, L. P. Regnault, J. Rossat-Mignod, J. P. Renard, J. Bouillot, W. G. Stirling, and F. Mezei, Physica **120B**, 241

(1983).
[31]J. P. Boucher, L. P. Regnault, J. Rossat-Mignod, J. Y. Henry, J. Bouillot, W. G. Stirling, E. A. Soares, J. Wiese, and J. P. Renard, *A travers la physique,* in *Les Editions de Physique* (Societé Française de Physique, Paris, 1984), p. 327.
[32]J. P. Boucher, L. P. Regnault, A. Pires, J. Rossat-Mignod, Y. Henry, J. Bouillot, W. G. Stirling, and J. P. Renard, in *Magnetic Excitations and Fluctuations,* edited by S. W. Lovesey, U. Balucani, F. Borsa, and V. Tognetti (Springer, Berlin, 1984).
[33]I. U. Heilman, J. K. Kjems, Y. Endoh, G. F. Reiter, G. Shirane, and R. J. Birgeneau, Phys. Rev. B **24**, 3939 (1981).
[34]J. P. Boucher, J. Magn. Magn. Mater. **15**, 687 (1980).
[35]A. S. T. Pires and M. E. Gouvea, J. Phys. C **17**, 4009 (1984).
[36]J. M. Loveluck, J. Phys. C **12**, 4251 (1979).
[37]K. Maki, Phys. Rev. B **24**, 3991 (1981).
[38]H. J. Mikeska, Phys. Rev. B **26**, 5213 (1982).
[39]P. S. Riseborough, Solid State Commun. **48**, 901 (1983).
[40]P. S. Riseborough, D. L. Mills, and S. E. Trullinger, J. Phys. C **14**, 1109 (1981).